

This is a non-peer reviewed preprint submitted to EarthArXiv.

This manuscript has been submitted for publication to Quaternary Science Reviews.

Any comments can be addressed to Jenni Robertson (j.robertson@praxisuk.co.uk)

Twitter: @GeoJenni

**$^{234}\text{U}/^{230}\text{Th}$ coral growth dating yields reliable ages in restricted basins despite
anomalous $\delta^{234}\text{U}_i$ values**

J. Robertson^{a*}, D. Sahy^b, G.P. Roberts^a, M. Meschis^{c,a}

^aDepartment of Earth and Planetary Sciences, Birkbeck College, University of London, WC1E 7HX, UK.

^bBritish Geological Survey, Keyworth, NG12 5GG, United Kingdom.

^cDepartment of Physics and Astronomy, University of Bologna, Viale Berti Pichat 8, 40127, Bologna, Italy

dihy@bgs.ac.uk gerald.roberts@ucl.ac.uk marco.meschis@unibo.it

Corresponding author: Jenni Robertson (jrober05@mail.bbk.ac.uk or j.robertson@praxisuk.co.uk)

1 Late Quaternary coral growth ages from uplifted coastal regions, such as marine terraces and
2 associated palaeoshorelines, are an essential tool used to derive tectonic and fault controlled uplift
3 and deformation rates, and thus contribute to seismic hazard analysis and constrain past global sea
4 levels. Fossil coral growth ages are assessed for reliability based upon whether the $\delta^{234}\text{U}_i$ (or initial
5 activity ratio $^{234}\text{U}/^{238}\text{U}$) matches the present-day oceanic value of $\sim 145 \pm 1.5\%$. However, $\delta^{234}\text{U}_i$ values
6 outside of this range have been measured from corals at palaeoshoreline locations throughout the
7 world (e.g. Greece, Italy, western USA; Iran) where the coral ages obtained are typically consistent
8 with glacio-eustatic sea-level highstand timing, their stratigraphic/tectonic settings and other age
9 constraints. We explore this controversy with a detailed analysis of coral growth ages from within the
10 semi-restricted Gulf of Corinth, where only 4% of 154 dated corals display $\delta^{234}\text{U}_i$ within $\pm 10\%$ of the
11 open ocean value but appear to have growth ages that agree with highstand timing, stratigraphy and
12 ages from ^{36}Cl exposure dating of wave-cut platforms. We undertook multiple $^{234}\text{U}/^{230}\text{Th}$ analyses on
13 individual corallites which are used in combination with analysis of existing coral growth age data and
14 $^{87}\text{Sr}/^{86}\text{Sr}$ values to suggest that $\delta^{234}\text{U}_i$ within the Gulf of Corinth was elevated throughout Marine
15 Isotope Stages 5e-7a (125-200 ka highstands), as a consequence of growth within a basin subject to
16 limited seawater entry during marine highstands and freshwater input from rivers and groundwater
17 combined with episodic fault uplift. Within the Gulf of Corinth, our findings are used to explore the
18 late Quaternary pattern of gulf-wide fault-related uplift, and suggest that where corals from marginal
19 coastal/restricted basins are dated, deviations in $\delta^{234}\text{U}_i$ from the open ocean value should be carefully
20 considered.

21 Keywords: Quaternary, Europe, U-Th series, corals, palaeoshorelines, tectonic uplift, $\delta^{234}\text{U}_i$

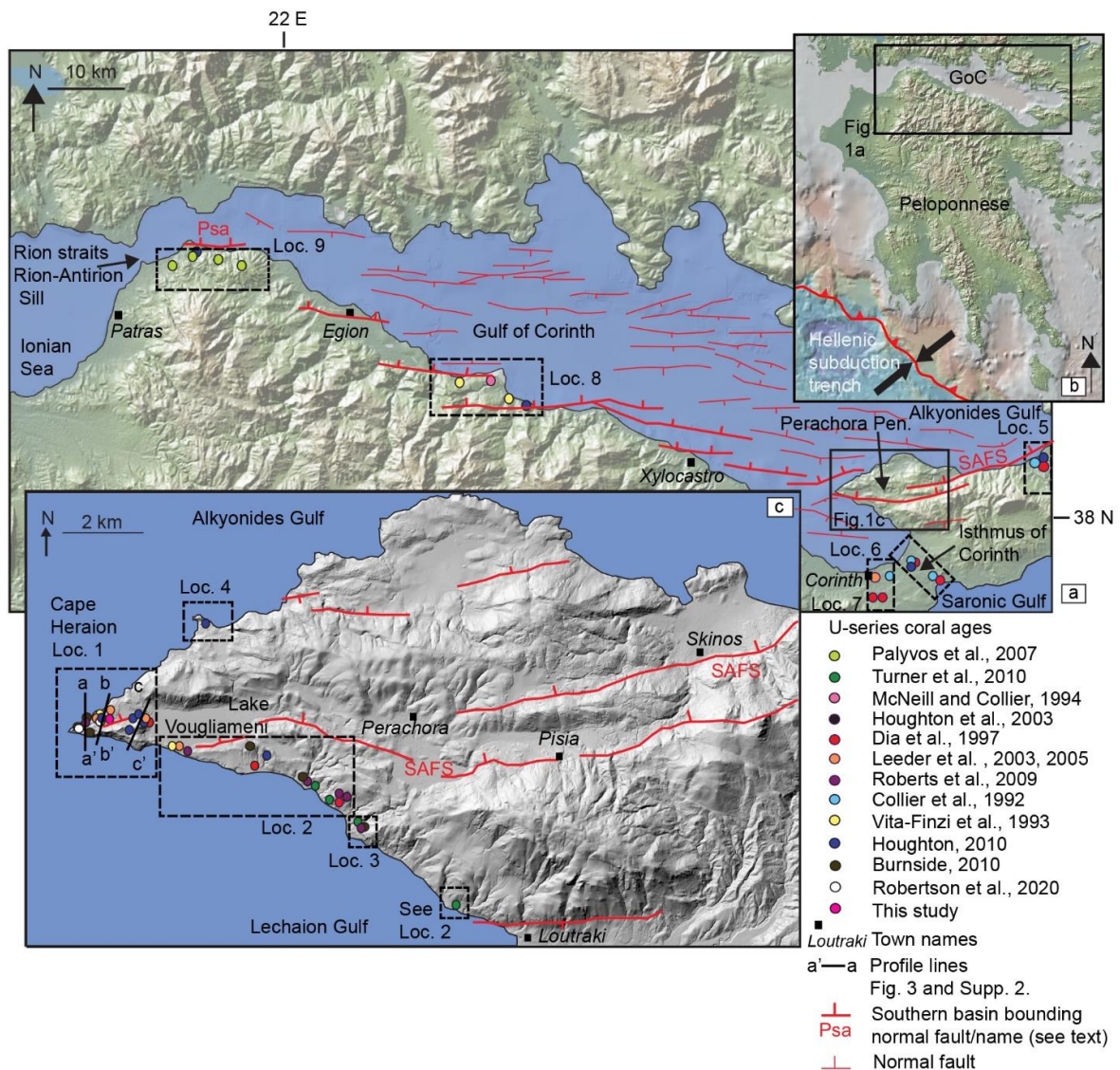
22 1. Introduction

23

24 U-series coral growth ages provide the foundation for the study of global sea level (e.g. Muhs et al.,
25 1994; Gallup et al., 1994) and derivation of uplift rates along tectonically-active coastal margins
26 because they provide numerical ages for palaeoshorelines (e.g. Muhs et al., 1994; Bard et al., 1996;
27 Grant et al., 1999; Houghton et al., 2003; Sieh et al., 2008; Roberts et al., 2009). This latter body of
28 work explores sequences of palaeoshorelines and shallow water coral reefs that have been uplifted
29 as a result of large and moderate earthquakes and thus contributes to seismic hazard analysis (e.g.
30 Grant et al., 1999; McNeill and Collier, 2004; Sieh et al., 2008; Roberts et al., 2009). The reliability of
31 fossil coral growth ages is predominantly evaluated based upon whether $\delta^{234}\text{U}_i$ is reflective of present-
32 day homogenous open ocean values ($\sim 145 \pm 10\%$) (e.g. Medina-Elizalde et al., 2013; Chutcharavan et
33 al., 2018); values that have previously been suggested to have not significantly deviated throughout
34 the late Quaternary (e.g. Hamelin et al., 1991). Late Quaternary $\delta^{234}\text{U}_i$ variation is usually attributed
35 to post-depositional diagenetic alteration reflective of open system behaviour since the coral formed
36 (Bard et al., 1991; Dutton, 2015).

37 The problem is that samples of shallow fossil corals used to infer uplift rates are typically obtained
38 from coastal margins and restricted basins, and have been shown to display $\delta^{234}\text{U}_i$ outside of the ~ 145
39 $\pm 10\%$ range (Chutcharavan et al., 2018), which some authors suggest limits their utility to provide
40 numerical age constraints (e.g. Bard et al., 1991; Hamelin et al., 1991; see Chutcharavan et al., 2018
41 for a discussion). Whilst corals from these settings display anomalous $\delta^{234}\text{U}_i$, in many cases their
42 growth ages are in agreement with other coral ages and age constraints, eustatic sea-level highstands
43 and expected stratigraphical settings consistent with the local tectonics (e.g. Muhs et al., 1994; Bard
44 et al., 1996; Grant et al., 1999; Roberts et al., 2009). It is suggested that corals from coastal margins
45 and restricted basins with anomalous $\delta^{234}\text{U}_i$ may represent systematic variation of $\delta^{234}\text{U}_i$ as a result of
46 spatial and temporal differences in water chemistry (Andersen et al., 2007; Esat and Yokoyama, 2010),
47 but actual examples and detailed investigations are few.

48 This study investigates new and existing $^{234}\text{U}/^{230}\text{Th}$ coral growth ages from within the Gulf of Corinth,
49 Greece, (Fig. 1) a semi-restricted marine basin (Perissoratis et al., 2000) affected by tectonics, glacio-
50 eustatic sea-level changes and influxes of freshwater from rivers and springs (Perissoratis et al., 2000;
51 Roberts et al., 2009; Houghton, 2010; Nixon et al., 2016). Coral growth ages from within the gulf have
52 elevated $\delta^{234}\text{U}_i$, but cluster on known glacio-eustatic highstands, agree with other absolute age
53 constraints and can be explained relative to their stratigraphic position. The findings of this study will
54 show that multiple $^{234}\text{U}/^{230}\text{Th}$ analyses on a number of corallites from the same sedimentary layers
55 reveals age and $\delta^{234}\text{U}_i$ clustering, suggestive of unaltered corals. Our results indicate that: (i) $^{234}\text{U}/^{230}\text{Th}$
56 analyses on corals from palaeoshorelines with $\delta^{234}\text{U}_i$ values that differ from present day open ocean
57 $\delta^{234}\text{U}_i$ warrants further investigation and, (ii) that the Late-Quaternary $\delta^{234}\text{U}_i$ of the Gulf of Corinth
58 may have been elevated with respect to open ocean $\delta^{234}\text{U}_i$ due to a combination of the tectonics of
59 the gulf, freshwater influx and eustatic variations of sea level. This outcome is used to explore patterns
60 of gulf-wide fault-displacement throughout the late Quaternary and to infer that the impact of
61 restricted basins and coastal margins on water uranium isotope composition, and therefore coral
62 $\delta^{234}\text{U}_i$, should be carefully assessed when considering the reliability of coral growth ages.



63

64 Figure 1: (a) Map of the Gulf of Corinth showing normal faults as per Nixon et al. (2016) and the locations of coral growth
 65 ages colour coded by study. (b) Location of the Gulf of Corinth within Greece. (c) Detailed map and coral growth locations
 66 on the Perachora Peninsula at the eastern end of the Gulf of Corinth (see Supplementary Fig. 1 for sampling locations for
 67 this study). Profile lines relate to cross sections in Fig. 3 and Supplementary Fig. 2. Locality references in (a) and (c) relate to
 68 Fig. 3, Supplementary Fig 2 and discussions in the text.

69

70 2. Background

71 2.1 The Gulf of Corinth

72

73 The Gulf of Corinth formed as a result of normal faulting in response to high extensional north-south
74 strain rates across central Greece; which continues to be active to the present day. Geodetic extension
75 rates of ~5-15 mm/yr (Clarke et al., 1998; Briole et al., 2000) are accommodated predominantly along
76 north-dipping faults that bound the southern margin of the gulf (Roberts et al., 2009; Nixon et al.,
77 2016) (Fig. 1a). The gulf is a bathymetrically-restricted marine embayment currently linked to the
78 Ionian Sea at its western end via the Rion Straits and at its eastern point via the human-made Corinth
79 Canal, which cuts through the Isthmus of Corinth (Fig. 1a). The hydrochemistry of the gulf is marine
80 and influenced by a combination of freshwater run-off from the surrounding mountains, local climate,
81 and the exchange of waters with the Ionian Sea above the Rion-Anterion sill along the Rion Strait,
82 which is 2 km wide and ~60 m deep (Perissoratis et al., 2000; McNeill et al., 2019).

83 Multiple seismic reflection studies, boreholes and recent cores from within the Gulf of Corinth provide
84 evidence of alternating lowstand (lake) and highstand (marine) deposits throughout the late
85 Quaternary (e.g. Perissoratis et al., 2000; Papanikolaou et al., 2015; McNeill et al., 2019). Recent
86 results from IODP mission 381 (site M0079) in the centre of the Gulf of Corinth shows that over the
87 past ~750 ka the gulf has experienced changing environmental conditions driven by climatic and
88 eustatic changes whereby a range of basin environments between the simple marine and freshwater
89 end-members occurred (McNeill et al., 2019). During sea level lowstands the gulf is dominated by
90 freshwater influx due to precipitation and run off (Perissoratis et al., 2000; Watkins et al., 2020). The
91 history of seawater ingress into the gulf during highstands is more complex, however, and has changed
92 throughout the late Quaternary as result of the relative motion of uplift and subsidence on normal
93 faults at the eastern and western ends of the gulf (Roberts et al., 2009; McNeill et al., 2019).

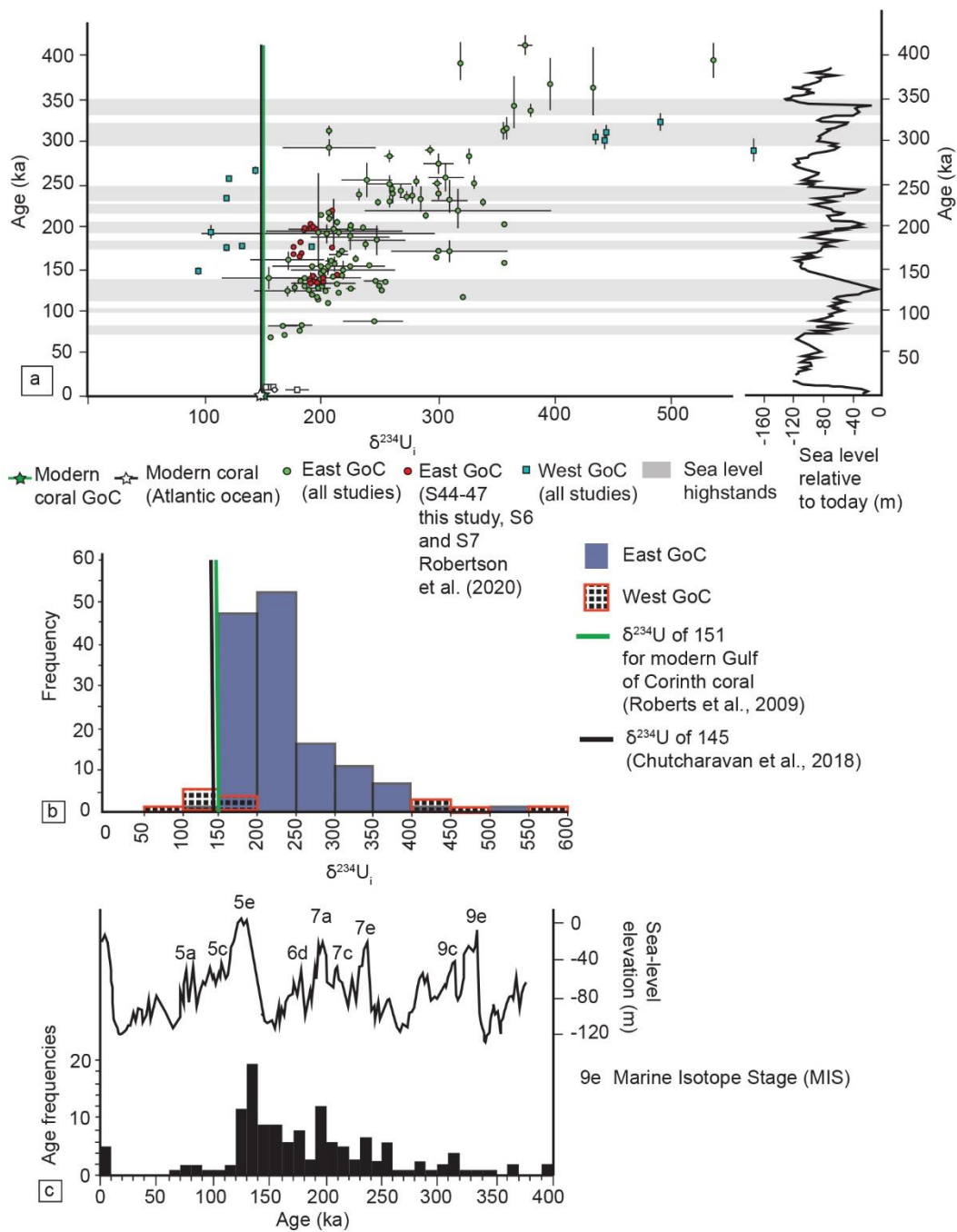
94 In particular, knowledge of highstand ages from sea-level curves combined with observations from
95 uplifted preserved marine terraces and palaeoshorelines throughout the gulf have been used to

96 explore the pattern of water ingress throughout the late Quaternary (Roberts et al., 2009). Roberts
97 et al. (2009) suggest that between 340 ka and ~150 ka the Rion-Anterion sill (western gulf, Fig. 1a) was
98 above relative sea level and that the Rion Strait became an inlet for seawater during Marine Isotope
99 Stage (MIS) 5e (125 ka highstand) due to hangingwall subsidence along the Psathopyrgos fault (Psa,
100 Fig. 1a) (Houghton et al., 2003; Roberts et al., 2009), resulting in a narrow and shallow channel
101 (Perissoratis et al., 2000). During this time seawater from the Saronic Gulf entered the Gulf of Corinth
102 via the narrow Isthmus of Corinth (Roberts et al., 2009) (Fig. 1a), evidenced by subaqueous dunes of
103 oolitic limestones (Collier and Thompson, 1991), late Quaternary corals (Collier et al., 1992; Dia et al.,
104 1997) and microfossil analysis from boreholes (Papanikolaou et al., 2015). The evolution of the
105 Isthmus of Corinth from a marine inlet to sub-aerial setting occurred sometime after MIS 5e (125 ka)
106 as a result of sustained footwall uplift of ~0.3-0.6 mm/yr due faulting along the South Alkyonides Fault
107 System (SAFS) (Roberts et al., 2009; Papanikolaou et al., 2015) (Fig. 1a).

108 2.2 Gulf of Corinth corals

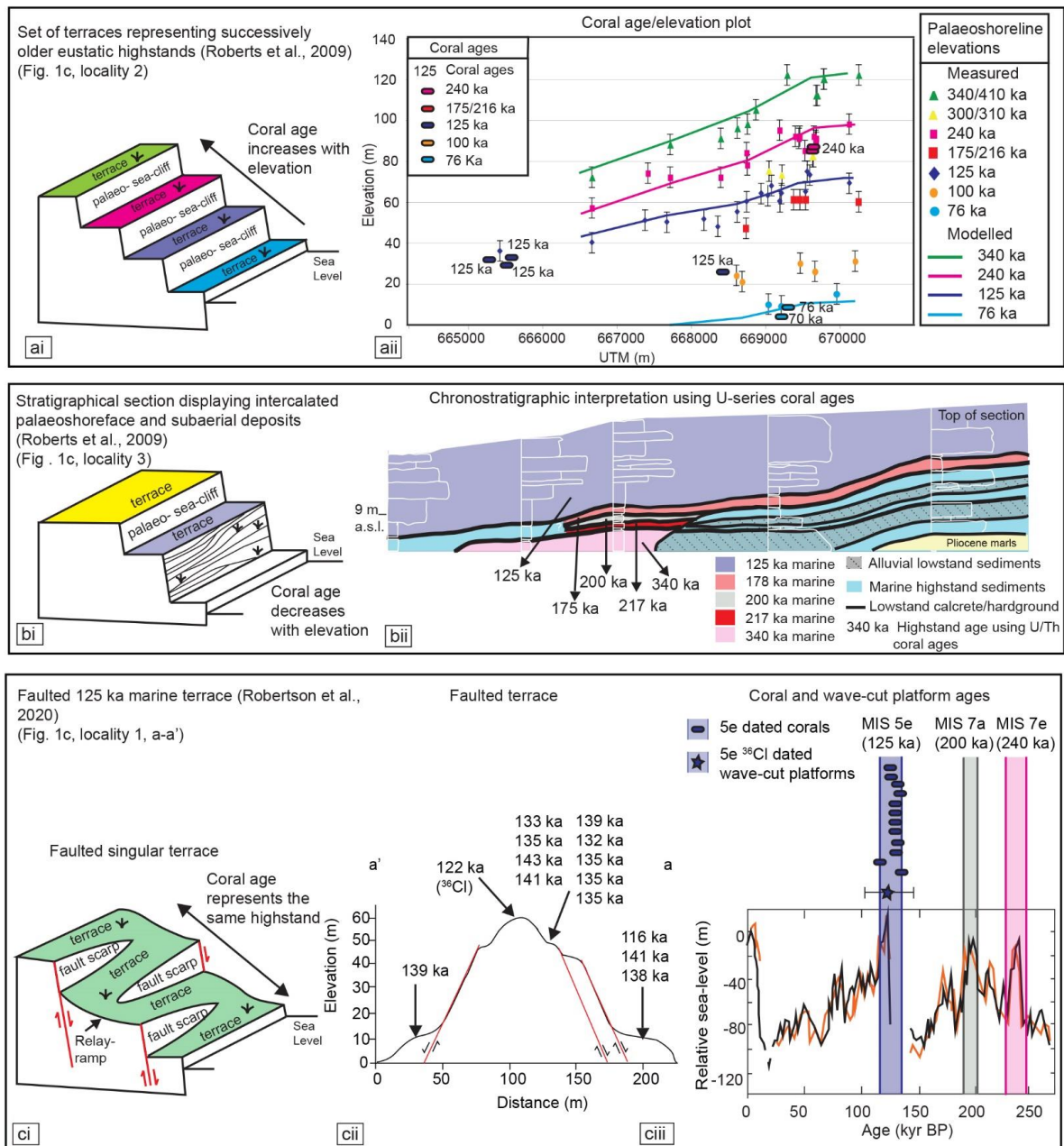
109 Coral growth ages sampled from the uplifted footwalls along the southern margin of the gulf (Fig. 1a,
110 c) typically have elevated $\delta^{234}\text{U}_i$ (Fig. 2a, b) (Collier et al., 1992; Vita-Finzi et al., 1993; Dia et al., 1997;
111 Houghton et al., 2003; Leeder et al., 2003; McNeill and Collier, 2004; Leeder et al., 2005; Palyvos et
112 al., 2010; Roberts et al., 2009; Burnside, 2010; Houghton, 2010; Turner et al., 2010; Robertson et al.,
113 2020). Previous studies have calculated fault-related uplift rates using coral ages to inform studies on
114 gulf-wide horizontal deformation over long term (10^{4-5} years) timescales and to analyse the behaviour
115 of normal faulting within an active rift system (e.g. Houghton et al., 2003; McNeill and Collier, 2004;
116 Roberts et al., 2009; Bell et al., 2011). Within these studies, coral growth age reliability has been based
117 upon growth ages that fit known eustatic sea-level highstands (e.g. Houghton et al., 2003; Leeder et
118 al., 2005; Roberts et al., 2009; Robertson et al., 2020) (Fig. 2a, c), are stratigraphically consistent with

119 observed and modelled palaeoshorelines along sequences of terraces (Fig. 3a) and palaeoshoreface
 120 sections (Fig. 3b) (Roberts et al., 2009), and have additional age controls that support coral growth
 121 ages, for example ^{36}Cl cosmogenic exposure dating of wave-cut platforms associated with coral growth
 122 (Robertson et al., 2020) (Fig. 3c).



124 Figure 2: (a) Coral growth ages and $\delta^{234}\text{U}_i$ values for the Gulf of Corinth (Collier et al., 1992; McNeill and Collier, 2004; Dia
125 et al 1997; Leeder et al., 2005; Roberts et al., 2009; Burnside, 2010; Houghton, 2010; Turner et al., 2010; Robertson et al.,
126 2020) including this study. All ages and $\delta^{234}\text{U}_i$ values have been recalculated according to the decay constants of Cheng et
127 al., 2013. Sea level curve in (c) adapted from Siddall et al. (2003). See Table 1 for MIS and sea-level highstand timing
128 sources. Where uncertainties are not shown, values are within symbol size or not provided from older studies. (b)
129 Histogram of the $\delta^{234}\text{U}_i$ values for coral ages from the east and west Gulf of Corinth. (c) Histogram of frequencies of Gulf of
130 Corinth coral growth ages compared to the sea-level curve of Siddall et al. (2003).

131 Corals from within the Gulf of Corinth are located in three tectonic/stratigraphic settings where
132 different age relationships between growth ages and elevation are observed: (i) sequences of uplifted
133 marine terraces and palaeoshorelines that form during glacio-eustatic highstands and are preserved
134 as a result of the interplay between sea-level change and fault-related uplift; here corals located on
135 sequences of terraces have growth ages that increase with elevation (Fig. 3a), (ii) stratigraphical
136 shoreface sections from shallow marine environments where vertically stacked coral colonies are
137 separated by lowstand exposure surfaces; these sections record the transition through late
138 Quaternary highstands and have coral ages that decrease upward through the stratigraphy (Fig. 3b),
139 and (iii) marine terraces that have experienced faulting since they were formed; here corals from the
140 same highstand are now located at different elevations having experienced relative subsidence or
141 uplift as a result of normal faulting (Fig. 3c). Taken together, these examples highlight the problem
142 explored in this study. Why is that coral growth ages that make sense with their stratigraphic setting
143 and coincide with known glacio-eustatic sea-level highstands, are associated with elevated $\delta^{234}\text{U}_i$
144 values?



145

146 Figure 3: Examples of coral growth ages from within the Gulf of Corinth that have multiple ages in agreement with
 147 highstand timescales (Table 1) and are in the correct stratigraphic order given their setting (see Fig. 1a for localities): (a)
 148 Locality 2 (i) Cartoon of the geomorphological setting of a sequence of marine terraces. (ii) Coral ages that increase with
 149 age representing successively older terraces as elevation increases. The coral ages agree with observed and modelled
 150 palaeoshoreline elevations, modified from Roberts et al. (2009). (b) Locality 3 (i) Cartoon of the geomorphological setting
 151 of stratigraphical section. (ii) Coral ages in a stratigraphic section recording the transitions between highstand and
 152 lowstands, coral growth ages become younger as elevation increases, modified from Roberts et al. (2009). (c) Locality 1,
 153 profile a'-a. (i) Cartoon of a faulted marine terrace with multiple corals at different elevations on Cape Heraion. (ii) Coral
 154 and ³⁶Cl wave cut platform ages that represent MIS 5e (125 ka highstand) and have been faulted from their original
 155 position, modified from Robertson et al. (2020). (iii) Coral and ³⁶Cl wave-cut platform ages plotted on the sea-level curve
 156 of Siddall et al., 2003 (note that orange and black lines represent curves obtained using different core data).

157

158 Previous work to explore the anomalously high $\delta^{234}\text{U}$ observed in Gulf of Corinth corals used analysis
159 of $^{87}\text{Sr}/^{86}\text{Sr}$ measured from the dated corals to explore whether the water chemistry of the gulf may
160 have differed during highstands (Dia et al., 1997; Houghton, 2010). Consistently low measurements of
161 $^{87}\text{Sr}/^{86}\text{Sr}$, relative to the present day in the Gulf of Corinth, were observed. Possible explanations for
162 low $^{87}\text{Sr}/^{86}\text{Sr}$ were cited as diagenetic processes (Dia et al., 1997) or freshwater influx from a carbonate
163 catchment area with low $^{87}\text{Sr}/^{86}\text{Sr}$ that altered the chemistry of the gulf (Burnside, 2010; Houghton,
164 2010).

165 With the exception of corals studied by Collier et al. (1992) that used *Acropora sp.*, all of the coral
166 growth ages from within the Gulf of Corinth are obtained from *Cladocora caespitosa*. *C. caespitosa* in
167 the Gulf of Corinth grew as isolated colonies rather than extensive reefs (Dia et al., 1997) and differ
168 from many other corals in that they thrive in coastal and brackish/fresh water environments because
169 they are able to tolerate alluvial inputs and higher turbidity (Peirano et al., 2004). Modern day *C.*
170 *caespitosa* occur in shallow water between 4-10 m in depth, but have been known to live down to
171 depths of 40 m (Peirano et al., 2004). Studies on *C. caespitosa* show they are a long-lived species with
172 slow growth rates of up to 3.08 mm/yr (Zunino et al., 2018).

173 **3. Approach and methods**

174 The accuracy of coral ages is dependent on: (i) knowledge of the decay constants of U-series nuclides,
175 (ii) the assumption that ^{230}Th was negligible at the time of coral growth and, (iii) the assumption that
176 closed system conditions prevailed whereby no further isotopic exchange occurred between the coral
177 and its surrounding environment (Dutton, 2015). This latter point is tested by comparing the $\delta^{234}\text{U}$ of
178 the sample to the $\delta^{234}\text{U}$ of the open ocean. While the first two points can be satisfied (see below), we

179 question whether the corals within this study formed in seawater with a $\delta^{234}\text{U}_i$ comparable to the
180 present day. To explore this, $^{234}\text{U}/^{230}\text{Th}$ analyses on corals from the same sedimentary layer on Cape
181 Heraion were undertaken, with multiple $^{234}\text{U}/^{230}\text{Th}$ analyses on each corallite. These new $^{234}\text{U}/^{230}\text{Th}$
182 coral ages were used in addition to data from multiple analyses on two corallites from a recent study
183 (Robertson et al., 2020) also from Cape Heraion (Fig. 1). The approach adopted herein assumes that
184 growth age robustness can be established if clustering of ages and $\delta^{234}\text{U}_i$ are observed from different
185 corallites and multiple analyses on the same corallite (Esat and Yokoyama, 2010), especially if the coral
186 age is consistent with independent geological constraints. Such clustering may be indicative of corals
187 displaying closed system behaviour, where $\delta^{234}\text{U}_i$ values are representative of the water chemistry at
188 the time of growth. The $\delta^{234}\text{U}_i$ of the samples dated herein and in Robertson et al. (2020) are then
189 used as the basis to investigate $\delta^{234}\text{U}_i$ on all late Quaternary corals dated within the Gulf of Corinth.

190 3.1 Recalculation of all coral ages and $\delta^{234}\text{U}$ values to the same decay constants

191 U-series ages of corals from all known studies from within the Gulf of Corinth were compiled (Collier
192 et al., 1992; Vita-Finzi et al., 1993; Dia et al., 1997; Houghton et al., 2003; Leeder et al., 2003; McNeill
193 and Collier, 2004; Leeder et al., 2005; Palyvos et al., 2010; Roberts et al., 2009; Burnside, 2010;
194 Houghton, 2010; Turner et al., 2010; Robertson et al., 2020) (n=154) (Fig. 2a; Supplementary Table 1).
195 As these studies have occurred over three decades, different decay constants of ^{230}Th and ^{234}U have
196 been used to calculate the activity ratios, and thus age and $\delta^{234}\text{U}_i$ of the coral samples. To compare
197 the coral ages and $\delta^{234}\text{U}_i$ values from different studies, we recalculated coral ages and $\delta^{234}\text{U}_i$ (as per
198 Dutton, 2015), using the decay constants of Cheng et al. (2013). Recalculation required the original
199 decay constants, activity ratios and/or isotope data, and resulted in changes of $\sim <1\%$ to most coral
200 growth ages (Supplementary Table 1). The original decay constants were not published in McNeill and
201 Collier (2004), the ages and $\delta^{234}\text{U}_i$ values have been recalculated assuming that the decay constants

202 of Edwards et al. (1987) were originally employed. However, a lack of reported measurement data for
203 Palyvos et al., 2010 and samples 89/1 and 89/4 from Vita-Finzi et al., 1993 mean that these coral age
204 data (n=10) cannot be recalculated and are therefore excluded from this study.

205 3.2 $^{234}\text{U}/^{230}\text{Th}$ dating

206 The results of new (samples 44-47) $^{234}\text{U}/^{230}\text{Th}$ and recent (Samples S6 and S7, Robertson et al., 2020)
207 analyses on *C. caespitosa* coral samples from Cape Heraion are used herein. Samples S6 and S7 (Figs.
208 1c Profile line a-a', 3c, Supplementary Fig. 1a, c, d, Supplementary Table 1) were removed from the
209 sandy layer on a MIS 5e (125 ka) wave-cut platform (44 m) constrained using ^{36}Cl exposure dating
210 (Robertson et al., 2020). Samples 44-47 were removed from a layer in a sedimentary succession (41
211 m) accessed via an ancient cistern (Fig. 1c Profile line b-b', Supplementary Fig. 1b, c, e). The sandy
212 layer of samples 44-47 occurs beneath a reported 125 ka wave-cut surface (Robertson et al., 2020)
213 and is comprised of whole and disarticulated fossils and coarse sand to pebble grain sizes, suggestive
214 of a high-energy environment.

215 Coral preparation and cleaning was carried out as per the method outlined in Roberts et al. (2009).
216 This involved fragmenting the coral, mechanical cleaning of the wall of the coral with a scalpel under
217 a microscope (discarding the septa) to remove areas of alteration and sediment, submerging the coral
218 in 10% hydrochloric acid for 2-3 seconds and rinsing in ultra-pure water. This process was repeated
219 until the coral was free from visible signs of alteration. Individual corallites were analysed and, for
220 selected corallites, multiple $^{234}\text{U}/^{230}\text{Th}$ analyses were carried out in order to assess for $\delta^{234}\text{U}$ clustering
221 and age reliability. $^{234}\text{U}/^{230}\text{Th}$ analysis was carried out according to the process outlined in Crémière et
222 al. (2016).

223 Standard methods for screening for anomalous ^{238}U and ^{230}Th were applied as per Dutton (2015).
224 Specifically, modern corals typically have uranium values $\sim 2\text{--}3.5$ ppm (Shen and Dunbar, 1995);
225 samples with significantly different values may be indicative of diagenetic processes and were
226 rejected. The $^{230}\text{Th}/^{232}\text{Th}$ ratio was checked to ensure that ^{230}Th was negligible during initial coral
227 growth, rejecting the sample if the value was too low (<100) (van Calsteren and Thomas, 2006) or the
228 concentration of ^{232}Th was too high (as identified by Dia et al. (1997) for their samples). These methods
229 of screening were applied to corals dated in this study and all existing coral data assessed
230 (Supplementary Table 1).

231 3.3 MIS and sea-level highstands

232 Coral ages are discussed in reference to MIS and respective glacio-eustatic highstands. Herein, we use
233 the highstand ages from Siddall et al. (2003) and the lengths of MIS obtained from a number of studies
234 (Table 1). The focus was on analysing coral growth ages associated with MIS 5e (125 ka), MIS 6d (175
235 ka) and MIS 7a (200 ka) (Table 1). MIS 5e is well studied and there is relative certainty that between
236 129-116 ka the sea-level was above the present day value (Dutton et al., 2015). However, it is expected
237 that coral growth in the gulf would have occurred when lake Corinth experienced sea-water ingress
238 following the penultimate glacial maximum (~ 150 ka), but the timing of this ingress is poorly
239 constrained. It is suggested that sea-level rise at the beginning of interglacial periods occurs quickly,
240 reaching maximum sea-level rise rates within ~ 2 kyrs of the onset of deglaciation (Grant et al., 2014).
241 For MIS 5e, Gallup et al. (2002) suggest that 80% of sea-level rise following the glacial period of MIS
242 6a (~ 150 ka) occurred before 135 ka. Analysis of the rates of sea-level rise from Grant et al. (2014)
243 suggests that from ~ 150 ka to ~ 138 ka sea level rise was 5-8 m/ky. An average rate of 6.5 m/ky is used
244 alongside the relative sea-level at 150 ka of -90 m, to suggest that by 138 ka sea-level within the gulf
245 may have been ~ -12 m (± 10 m) relative to the present day. We suggest that it is plausible that coral

246 growth at this time could have occurred so 138 ka is used as an approximate age to indicate the
 247 beginning of MIS 5e in relation to the gulf.

MIS (highstand)	MIS time period (ka)	References
5a (76 ka)	70-82	N/A (used highstand age from Siddall et al., 2003, ± 6 ka error)
5c (100 ka)	94-106	N/A (used highstand age from Siddall et al., 2003, ± 6 ka error)
5e (125 ka)	116-138	Grant et al., 2014
6d (175 ka)	169-181	N/A (used highstand age from Siddall et al., 2003, ± 6 ka error)
7a (200 ka)	188-202	Dutton et al., 2009
7c (217 ka)	206-217	Dutton et al., 2009
7e (240 ka)	231-249	Dutton et al., 2009
9c (310 ka)	282-312	Rohling et al., 1998
9e (340 ka)	322-340	Rohling et al., 1998
11c (410 ka)	384-412	Rohling et al., 1998

248

249 Table 1: References used to inform the highstand time period within this study, where such data was not available, the
 250 highstand age ± 6 ka uncertainty from Siddall et al. (2003) was applied. See text for discussion on MIS 5e (125 ka) timing.

251

252 **4. Results and discussion**

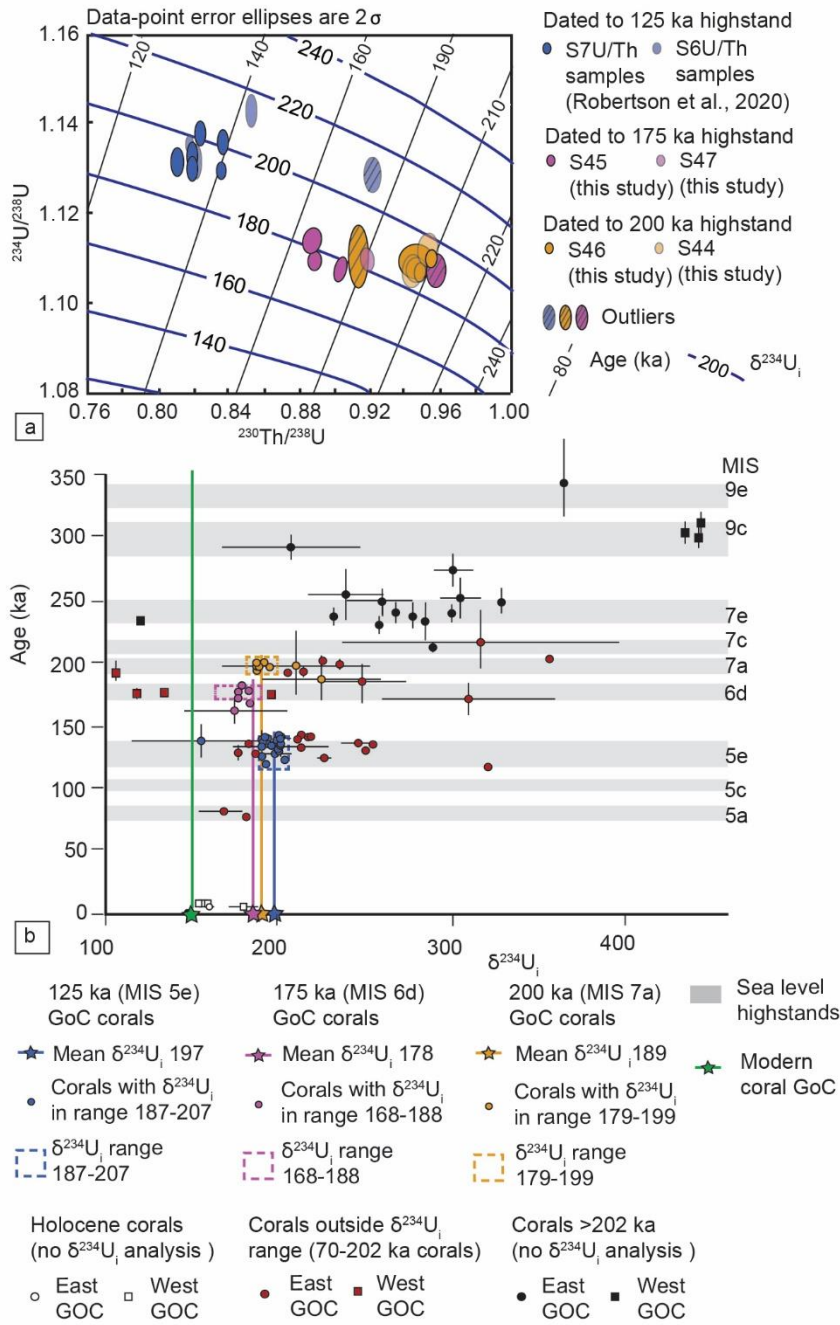
253 Coral growth ages and $\delta^{234}\text{U}_i$ from 22 coral samples (this study: 12, Robertson et al., 2020: 10) are
 254 discussed and used to suggest tentative $\delta^{234}\text{U}_i$ values for the Gulf of Corinth from MIS 5e to MIS 7a.
 255 Existing Gulf of Corinth coral ages are then investigated using: (i) the tentative $\delta^{234}\text{U}_i$ values, (ii) the
 256 tectonic/stratigraphic settings from which the corals were sampled and, (iii) their spatial relationship
 257 relative to other coral ages or age constraints. The outcome of this analysis suggests that the growth
 258 ages of corals are consistent with ages expected given their stratigraphic position and, therefore,
 259 elevated $\delta^{234}\text{U}_i$ is representative of late Quaternary hydrochemistry of the gulf. These findings are
 260 discussed in the context of the gulf-wide uplift rates and use of coral growth ages to derive uplift rates
 261 in coastal margins and restricted basins.

262 4.1 $\delta^{234}\text{U}_i$ during MIS 6d (175 ka) and 7a (200 ka)

263 The results of coral age dating on samples 44-47 (Fig. 1c: Locality 1, Profile line b-b'), removed from
264 the same sedimentary layer (Supplementary Fig. 1b, c, e), reveal ages and $\delta^{234}\text{U}_i$ values of multiple
265 analyses on 4 corallites (Fig. 4a, Table 2). Ages from corallites S44 (198 \pm 1.7 ka, 195 \pm 3.0 ka, 196 \pm 2.8
266 ka, 197 \pm 2.9 ka) and S46 (200 \pm 1.6 ka, 179 \pm 3.6 ka, 196 \pm 4.9 ka) suggest formation during the 200 ka
267 highstand (Table 1), the 179 ka sample has a low uranium value of 1.56 ppm and is disregarded (Table
268 2). Ages from corallite S45 (175 \pm 1.3 ka, 165 \pm 1.9 ka, 168 \pm 1.5 ka, 203 \pm 2.8 ka) and S47 (181 \pm 1.6 ka)
269 suggest formation during the 175 ka highstand (Table 1) where the 203 ka age is likely to be an outlier
270 and the 165- ka dated sample may be questionable owing to a low uranium value of 1.82 ppm (Table
271 2). As described above, corals 44-47 were located below the 125-ka wave-cut platform, so coral ages
272 older than this are not unexpected.

273 In other words, the ages of samples 44-47 are expected when their geological setting is considered;
274 sampled from the same bioclastic-rich layer, the corals occur stratigraphically below a 125 ka (MIS 5e)
275 ^{36}Cl exposure dated wave-cut surface (Supplementary Fig. 1b, c, e) (Robertson et al., 2020). The
276 presence of 175 ka and 200 ka corals in this location can be explained by the following sequence of
277 events, invoking erosion and isolation of whole corallites followed by re-sedimentation, using the sea
278 level curve of Siddall et al. (2003) (elevations are relative to sea level today): (i) coral samples 44 and
279 46 grew during MIS 7a (200 ka highstand) below the -5 m (\pm 12 m) maximum sea level at this time, (ii)
280 sea-level fell during lowstand MIS 6e to beyond \sim -60 m; (iii) sea-level rose to a maximum of \sim -30 m (\pm
281 12 m) within MIS 6d (175 ka highstand), during which the growth of samples 45 and 47 occurred, and
282 was followed by a fall in sea level to between -60 m to -80 m during MIS 6c-6a; (iv) the subsequent
283 125 ka highstand (MIS 5e) resulted in sea level rise to \sim 5 m (\pm 12 m) and a wave-cut platform was
284 formed. This substantial sea-level rise could have eroded the coral colonies of 200 ka and 175 ka from

285 their growth positions and deposited the corallites in their present day location within possible MIS
286 5e-aged sediments, following which the wave-cut platform formed. Preservation of the wave-cut
287 platform and associated coral samples are as a consequence of sustained fault-controlled uplift since
288 ~125 ka (Robertson et al., 2020). The above scenario suggests an uplift rate of 0.41 mm/yr, a value
289 that is similar to those proposed for this location (Robertson et al. 2020), and is hence not
290 unreasonable.



291

292 Figure 4: (a) U-Th evolution diagram with the results of dating on samples 44-47 (this study) and S6 and S7 (Robertson et
 293 al., 2020). (b) Plot of all acceptable (see text for detail) highstand coral growth ages from within the Gulf of Corinth. For
 294 samples 70-202 ka, colour coding is according to whether the sample has $\delta^{234}\text{U}_i$ within the range identified in this study.
 295 Holocene corals and corals ≥ 203 ka are not evaluated on the basis of their $\delta^{234}\text{U}_i$. See Table 1 for detail of the sea-level
 296 highstand periods and Supplementary Fig. 2 for analysis for each locality.

297

298

Sample ref.	Age (ka)	$\pm 2s$ (abs) (ka)	U (ppm)	$(^{230}\text{Th}/^{232}\text{Th})$	$(^{232}\text{Th}/^{238}\text{U})$	$\pm 2s$ (%)	$(^{230}\text{Th}/^{238}\text{U})$	$\pm 2s$ (%)	$(^{234}\text{U}/^{238}\text{U})_m$	$\pm 2s$ (%)	$\delta^{234}\text{U}_i$
S44(1)	197.8	1.7	1.91	488.1	0.0019	0.06	0.948	0.25	1.107	0.16	187
S44(2)	195.3	3.0	2.05	379.7	0.0025	0.35	0.943	0.49	1.107	0.27	186
S44(3)	196.1	2.8	2.02	354.2	0.0027	0.36	0.945	0.48	1.108	0.21	187
S44(4)	196.9	2.9	1.91	274.4	0.0035	0.35	0.951	0.47	1.112	0.25	196
S45(1)	174.7	1.3	2.08	159.3	0.0057	0.05	0.903	0.31	1.108	0.20	176
S45(2)	165.0	1.9	1.82	281.8	0.0031	0.34	0.887	0.47	1.114	0.21	182
S45(3)	167.6	1.5	2.06	549.9	0.0016	0.45	0.889	0.35	1.110	0.16	176
S45(4)	203.1	2.8	2.64	213.4	0.0045	0.29	0.957	0.41	1.107	0.27	191
S46(1)	199.5	1.6	1.93	288.9	0.0033	0.05	0.954	0.26	1.110	0.15	193
S46(2)	178.5	3.6	1.56	385.9	0.0024	0.68	0.914	0.58	1.110	0.50	183
S46(3)	195.7	4.9	1.98	235.4	0.0040	0.82	0.946	0.87	1.110	0.30	190
S47(1)	181.2	1.6	1.92	526.4	0.0017	0.06	0.918	0.29	1.110	0.18	183

299

300 Table 2: $^{234}\text{U}/^{230}\text{Th}$ coral age dating analytical results for all samples 44-47 (this study) - activity ratios calculated using the
301 ^{234}U and ^{230}Th decay constants of Cheng et al. (2013). Activity ratios corrected for ^{230}Th , ^{234}U and ^{238}U contribution from the
302 synthetic ^{236}U - ^{229}Th tracer, instrument baselines, mass bias, hydride formation and tailing. ^{230}Th blanks amounting to $0.15 \pm$
303 0.03 fg were subtracted from each sample. ^{238}U blanks were on the order of 10 pg, and were negligible relative to sample
304 size. Age and $\delta^{234}\text{U}$ data were corrected for the presence of initial ^{230}Th assuming an initial isotope composition of
305 $(^{232}\text{Th}/^{238}\text{U}) = 1.2 \pm 0.6$, $(^{230}\text{Th}/^{238}\text{U}) = 1 \pm 0.5$ and $(^{234}\text{U}/^{238}\text{U}) = 1 \pm 0.5$ (all uncertainties quoted at the 2σ level).

306 Given the above scenario for the deposition of the corals and the fact that coral ages fall into sea-level
307 highstand periods, we suggest that these ages appear to be reliable. The $\delta^{234}\text{U}_i$ values of samples S44-
308 47 suggest that for the 200 ka highstand (MIS 7a) (S44, S46), $\delta^{234}\text{U}_i$ values range between 186-196. For
309 the 175 ka highstand (MIS 6d) (S45, S47), $\delta^{234}\text{U}_i$ values appear to have been between 176-183. All of
310 these values are higher than that of the present day oceans ($\sim 145\text{‰}$), but similar to the values
311 reported in other Gulf of Corinth corals (Fig. 3a; Supplementary Table 1). Differing $\delta^{234}\text{U}_i$ values for
312 each highstand within the Gulf of Corinth can be tentatively suggested using the mean of values from
313 the new coral ages herein. These values and their $\pm 10\text{‰}$ range (Fig. 4b) are 189‰ (179-199) for the
314 200 ka highstand (MIS 7a) and 178‰ (168-188) for the 175 ka highstand (MIS 6d).

315 4.2 $\delta^{234}\text{U}_i$ during MIS 5e (125 ka)

316 The coral ages of samples S6 and S7 sampled from 44 m on Cape Heraion (published in Robertson et
317 al., 2020) (Fig. 1c Profile a-a'; Fig. 4a; Supplementary Table 1; Supplementary Fig. 1a, c, d) suggest
318 growth during MIS 5e (125 ka highstand). These results are in agreement with coral growth ages from
319 other studies sampled from Cape Heraion (Fig. 1c) (Vita Finzi et al., 1993; Leeder et al., 2003; Leeder
320 et al., 2005; Roberts et al., 2009; Burnside, 2010; Houghton, 2010), all of which can be mapped into
321 wave-cut platforms dated to the 125 ka highstand (MIS 5e) using *in-situ* ^{36}Cl exposure dating
322 (Robertson et al., 2020) (Figs. 1c, 3c, Supplementary Fig. 1a, c, d). Examination of the multiple analyses
323 of samples S6 and S7 reveal seven growth ages reflective of MIS 5e (125 ka highstand) (Fig. 4a,
324 Supplementary Table 1) within the range 132-138 ka, two growth ages just outside the MIS 5e range
325 of 141 ± 0.8 ka and 143 ± 1.3 ka that we include in our analysis and an age of 174 ± 2 ka (S6) that appears
326 to be an outlier from analysis of corallite S6 and is herein excluded. The nine ages within the range of
327 132-143 ka all have acceptable uranium concentration levels and ($^{230}\text{Th}/^{232}\text{Th}$) values. $\delta^{234}\text{U}_i$ values of
328 samples S6 and S7 cluster between 191-214 (Fig. 4a) (mean of 197‰, and a ± 10 ‰ range of 187-207).
329 If the growth ages of 141 ka and 143 ka are excluded, then corals with growth ages between 132-138
330 ka have similar $\delta^{234}\text{U}_i$ values that cluster between 191-202 with a mean of 196‰.

331 In summary, comparing the $\delta^{234}\text{U}_i$ values of multiple analyses on individual corallites reveals elevated
332 values for MIS 5e (125 ka), MIS 6d (175 ka) and MIS 7a (200 ka) of 197‰, 178‰ and 189‰,
333 respectively, but growth ages that make sense with their stratigraphic and structural positions
334 (Supplementary Fig. 2). The ages within each highstand appear to broadly cluster together (Fig. 4a,
335 Supplementary Fig. 3). This observed clustering of samples within and between corallites is taken as
336 evidence that the $\delta^{234}\text{U}_i$ values may be representative of corals that formed during MIS 5e, 6d and 7a.
337 Alternatively, if the elevated $\delta^{234}\text{U}_i$ were caused by diagenesis then it may be expected that sub-
338 samples of the same corallite might have significantly different isotopic compositions, hence clustered
339 values would be unlikely. The similarity of both age and $\delta^{234}\text{U}_i$ values allows for a tentative suggestion

340 that the $\delta^{234}\text{U}_i$ of the Gulf of Corinth during late Quaternary highstands was higher than that of present
341 values and within the broad range of 160-217.

342 4.3 Coral ages and $\delta^{234}\text{U}_i$ values within their tectonic setting

343 Assuming that our late Quaternary $\delta^{234}\text{U}_i$ values highlighted above are correct, they are applied to the
344 recalculated coral age dataset (n=154) from within the Gulf of Corinth (Fig. 4b; Supplementary Table
345 1). However, prior to further analysis we exclude a number of samples (n=66), detailed in
346 Supplementary Table 1 and its caption. Plotting the age versus $\delta^{234}\text{U}_i$ of the remaining acceptable
347 samples (n=88) shows growth ages that cluster within glacio-eustatic highstand periods; however, we
348 note that samples have $\delta^{234}\text{U}_i$ values that fall within and outside of the $\delta^{234}\text{U}_i$ range identified herein
349 (for ages 69-202 ka) (Fig. 4b). Detailed analysis on the 88 acceptable samples reveals 5 samples that
350 have Holocene ages, 64 samples that have highstand ages between 69-202 ka (76-200 ka highstands,
351 Fig. 4b, Supplementary Table 1) with the remaining 19 samples ≥ 203 ka (Fig. 4b). Exploring the 64
352 samples with highstand growth ages between 69-202 ka, we examine whether the $\delta^{234}\text{U}_i$ values are
353 consistent with the ranges identified in Section 4.2. This shows that for the corals with 200 ka
354 highstand (MIS 7a) ages (n=16), 50% have $\delta^{234}\text{U}_i$ within the range of 179-189. For the corals with 175
355 ka highstand (MIS 6d) ages (n=11), 45% have $\delta^{234}\text{U}_i$ within the range of 168-188. For the corals with
356 125 ka highstand (MIS 5e) ages (n=35), 63% have $\delta^{234}\text{U}_i$ within the range of 187-207. However, note
357 that the remaining corals with $\delta^{234}\text{U}_i$ outside of these ranges have growth ages and sample locations
358 that fit with the stratigraphical and tectonic relationships in addition to agreeing with other coral ages
359 sampled from the same location (Supplementary Fig. 2), suggesting that acceptable $\delta^{234}\text{U}_i$ values may
360 have an even wider range that we specify in Section 4.2, perhaps due to relatively variable water
361 chemistry in some locations. Coral growth ages ≥ 203 ka (n=19) predominantly exhibit higher $\delta^{234}\text{U}_i$
362 that could be due to diagenetic processes or again may be an indication of different hydrochemistry

363 within the gulf at the time of growth. A lack of further analyses on these corals precludes further
364 explanation for ≥ 203 ka corals. Overall, these results suggest that $\delta^{234}\text{U}_i$ may have been elevated
365 during coral growth between 76-202 ka, but they also indicate that within the Gulf of Corinth there
366 appears to have been some spatial and temporal variability of $\delta^{234}\text{U}_i$.

367 We observe that 83% coral growth ages come from the eastern Gulf of Corinth (Figs. 1a, c,
368 Supplementary Table 1), and that all of the MIS 5e (125 ka highstand) dated corals are located in the
369 eastern Gulf of Corinth. One possible explanation for this is that coral growth is reflective of the
370 dominant seawater entry point during the highstands, but we do not discount that this could simply
371 be related to sampling and/or preservation bias. If the interpretation of seawater entry via the Rion
372 Straits and Isthmus of Corinth during MIS 5e proposed by Roberts et al. (2009) is accepted, restricted
373 seawater entry via the Rion Straits did not occur until sea level was near its maximum elevation
374 (stillstand) around 125 ka (MIS 5e). Prior to the MIS 5e stillstand, seawater entry would be
375 predominantly via the shallow Isthmus of Corinth into the eastern part of the gulf ~ 110 km to the east,
376 and coincidental to the location of all of the MIS 5e corals within this study. Further analysis shows
377 that 75% of MIS 5e corals (with $\delta^{234}\text{U}_i$ within the acceptable range determined herein) were dated to
378 the earlier part of the highstand from 138 ka to 125 ka (Supplementary Table 1) which could be used
379 to suggest that marginal water conditions during the early highstand favoured growth of *C. caespitosa*.
380 The coral growth ages herein can be inferred to suggest that sea-level rise during ~ 143 -138 ka was
381 high enough to enter through the Isthmus of Corinth and begin the transition from lake to marine
382 conditions.

383 4.4 Variable chemistry of the Gulf of Corinth throughout the Late Quaternary

384 Our interpretation that the Late Quaternary Gulf of Corinth $\delta^{234}\text{U}_i$ value was elevated with respect to
385 that of the open ocean is consistent with descriptions of the geological setting of other authors (Collier

386 et al., 1992; Roberts et al., 2009; Burnside, 2010; Houghton, 2010). The hypotheses of elevated $\delta^{234}\text{U}_i$
387 centres around transitions between a lake and semi-restricted marine basin throughout the Late
388 Quaternary as a result of the interplay between eustatic sea-level variation, freshwater influx and
389 fault-related subsidence/uplift along the Rion-Anterion sill and Isthmus of Corinth, respectively (Fig.
390 1a) (e.g. Roberts et al., 2009). Restricted/silled basins have been shown to have distinctive
391 hydrochemistry compared to that of the open ocean (Middelburg et al., 1991; Andersson et al., 1995;
392 Esat and Yokoyama, 2010). However, temporal and spatial variations of the hydrochemistry within the
393 faulted Gulf of Corinth basin are poorly understood. We know that marine conditions prevail at
394 highstands (Roberts et al., 2009; McNeill et al., 2019) and that during the transition from lowstand to
395 highstand the gulf is likely to become marine with a significant freshwater content (Perissoratis et al.,
396 2000), evidenced by highly variable microfossil assemblages that reveal complex basin environmental
397 variation between highstand and lowstand intervals (Roberts et al., 2009; McNeill et al. 2019). Little
398 else is known about the water chemistry, which is expected to be spatially and temporally variable
399 considering that: (i) the seawater inlets were narrow, shallow and changing over time (Collier and
400 Thompson, 1991; Perissoratis et al., 2000), (ii) sea level rises are spatially complex and may be non-
401 linear through time (e.g. Dutton et al., 2015), (iii) late Quaternary cyanobacterial mounds that
402 dominate Cape Heraion at Locality 1 (Fig 1. c) may provide evidence of rising groundwater altering the
403 water chemistry (Portman et al., 2005), and (iv) coral growth occurs in the footwalls along coastal
404 margins (localities 2-9, Fig. 1a) that are subject to episodic fault-related uplift and freshwater influx
405 from rivers and groundwater (Luijendijk et al., 2020). A study of the Holocene coastal marginal marine
406 environment along the southern western Gulf of Corinth (Soter et al., 2001) provides an analogue to
407 conditions during previous highstands. Spatial and temporal variations in hydrogeochemistry were
408 evidenced by complex sedimentology and stratigraphy suggestive of repeated transitions between
409 freshwater and brackish to marine conditions over periods of 1-3 ka due to a combination of tectonic

410 uplift, river drainage and the variation between rapid and decelerated sea-level rise (Soter et al.,
411 2001).

412 In summary, we propose that along the fault-controlled coastal margins of the Gulf of Corinth, the
413 dominant factor controlling the $\delta^{234}\text{U}_i$ of corals during previous highstands may be restricted seawater
414 entry into the gulf combined with freshwater influx from groundwater (Locality 1) and rivers (localities
415 2-9) (Fig. 1). The $\delta^{234}\text{U}_i$ of both groundwater and riverine input is dependent on the lithology of the
416 host rocks in the catchment or circulation area (Palmer and Edmond, 1993), which are predominantly
417 comprised of Mesozoic limestone and carbonate lithologies in the Gulf of Corinth (IGME, 1993). In the
418 eastern Gulf of Corinth, at Cape Heraion (Fig. 1c, Locality 1) the presence of high Mg/Sr cyanobacterial
419 mounds is interpreted as evidence that groundwater from submarine springs percolating along normal
420 faults was partially equilibrated with Mesozoic limestones, which have relatively high $\delta^{234}\text{U}_i$
421 (Houghton, 2010). This is relevant given that 18 of the coral samples from within Locality 1 are located
422 on or directly adjacent to these cyanobacterial mounds. In terms of the riverine input (localities 2-9,
423 Fig. 1) there are presently ~47 major rivers that drain into the southern gulf (Watkins et al., 2020), one
424 would expect that many of these also drained into the Gulf of Corinth throughout the late Quaternary.
425 Lithological, climatic and seasonal differences mean that riverine $\delta^{234}\text{U}_i$ may be highly variable in
426 comparison to seawater, where studies into individual rivers worldwide report significantly higher
427 values beyond 400-500 (e.g. Andersson et al., 1995; Andersen et al., 2007; Grzymko et al., 2007, and
428 *references therein*). While no such data exists for the Gulf of Corinth rivers, spatial and seasonal
429 temporal variation of $\delta^{234}\text{U}_i$ due to riverine input and restricted circulation has been observed in other
430 restricted basins such as the Baltic Sea (Andersson et al., 1995). Furthermore, a recent study by
431 Luijendijk et al. (2020) suggested that coastal groundwater discharge (a combination of submarine
432 and nearshore terrestrial groundwater discharge) takes place in a zone that extends 400 m from the

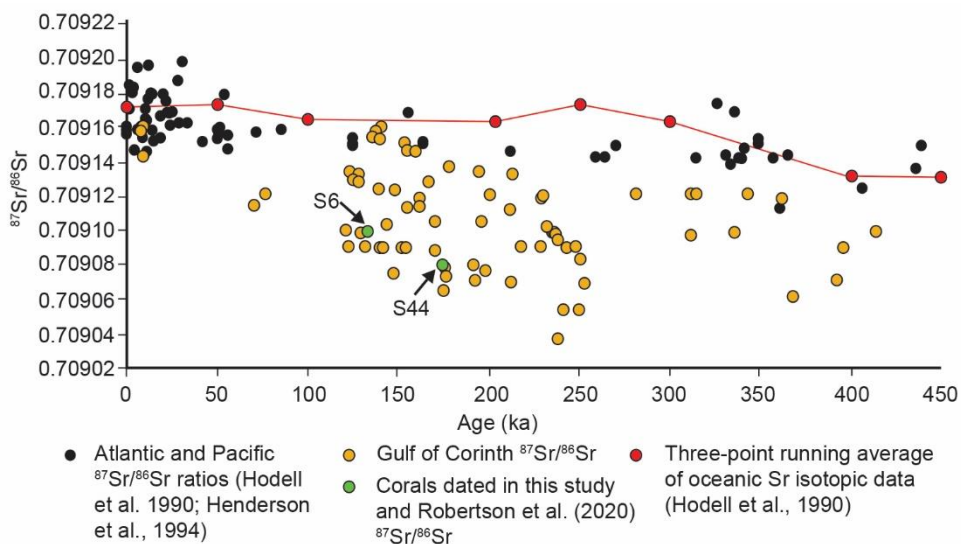
433 shore, and that due to spatial variability, this groundwater discharge can significantly impact coastal
434 hydrology.

435 4.4.1 Analysis of $^{87}\text{Sr}/^{86}\text{Sr}$ ratios throughout the Late Quaternary

436 A test of the hypothesis of elevated $\delta^{234}\text{U}_i$ of Gulf of Corinth corals as a direct consequence of
437 freshwater input can be carried out by investigating $^{87}\text{Sr}/^{86}\text{Sr}$ ratios. Corals and other marine carbonate
438 organisms record the $^{87}\text{Sr}/^{86}\text{Sr}$ ratios of the water in which they formed. Marine $^{87}\text{Sr}/^{86}\text{Sr}$ ratios have
439 been shown to be increasing quasi-linearly over the past 2.5 Ma, but exhibit less variation on
440 timescales over hundreds of thousands of years (Hodell et al., 1990). Present day homogenous
441 oceanic $^{87}\text{Sr}/^{86}\text{Sr}$ values (Hodell et al., 1990) and Gulf of Corinth values (Houghton, 2010) display values
442 of ~ 0.70917 . If freshwater influx dominated conditions along coastal margins, the $^{87}\text{Sr}/^{86}\text{Sr}$ chemistry
443 of the corals should reflect these conditions. However, this assumption is initially flawed because the
444 significant difference between Strontium (Sr) concentrations of riverine and oceanic waters, 1.0-4.0
445 μM and 90 μM respectively, means that riverine input into marginal seas may be unlikely to alter the
446 Sr concentrations (Krabbenhoft et al., 2010). The exception is in carbonate organisms grown in
447 brackish/low salinity environments, where the $^{87}\text{Sr}/^{86}\text{Sr}$ chemistry of the water may be significantly
448 affected by the freshwater $^{87}\text{Sr}/^{86}\text{Sr}$ (Bryant et al., 1995). Brackish/oligohaline conditions throughout
449 the Holocene and late Quaternary are evident from detailed observations on microfossils (Soter et al.,
450 2001; Roberts et al., 2009; Papanikolaou et al., 2015; McNeill et al., 2019). Consequently, we suggest
451 that the $^{87}\text{Sr}/^{86}\text{Sr}$ of corals from the Gulf of Corinth corals may be a reliable proxy to investigate the
452 observed elevated $\delta^{234}\text{U}_i$.

453 The $^{87}\text{Sr}/^{86}\text{Sr}$ ratio of freshwater is directly influenced by the dominant lithology of their
454 circulation/catchment areas (e.g. Palmer and Edmond, 1993; Hodell et al., 1990). Limestones and
455 other carbonate lithologies, which dominate the gulf, have low $^{87}\text{Sr}/^{86}\text{Sr}$ ratios, with worldwide values

456 of 0.707-0.709 (Burke et al., 1982) and Triassic limestones of the Perachora Peninsula (Fig. 1a)
 457 measured as 0.70771 (Houghton, 2010). Comparison of the $^{87}\text{Sr}/^{86}\text{Sr}$ ratios for corals from the Gulf of
 458 Corinth to those from the Pacific and Atlantic throughout the late Quaternary reveals that the Gulf of
 459 Corinth corals exhibit a range of $^{87}\text{Sr}/^{86}\text{Sr}$ ratios, that are moderately to significantly lower than Atlantic
 460 and Pacific levels from ~75 ka to ~350 ka (Fig. 5). Low $^{87}\text{Sr}/^{86}\text{Sr}$ on Gulf of Corinth corals was also
 461 observed by Dia et al. (1997) who considered that sample impurities and/or diagenetic processes may
 462 be the cause, however, Houghton, (2010) carried out detailed chemical analysis on meticulously
 463 cleaned corals and dismissed this explanation. We tentatively suggest that the observed elevated
 464 $\delta^{234}\text{U}_i$ in corals may be related to the same processes that produced the low $^{87}\text{Sr}/^{86}\text{Sr}$ ratios, but this
 465 needs further work.



466

467 Figure 5: $^{87}\text{Sr}/^{86}\text{Sr}$ and age plot for the Gulf of Corinth from corals assessed within this study against those from Hodell et
 468 al. (1990) from the Atlantic and Pacific, in addition to a worldwide Sr curve obtained from a three-point running average
 469 (Hodell et al., 1990).

470

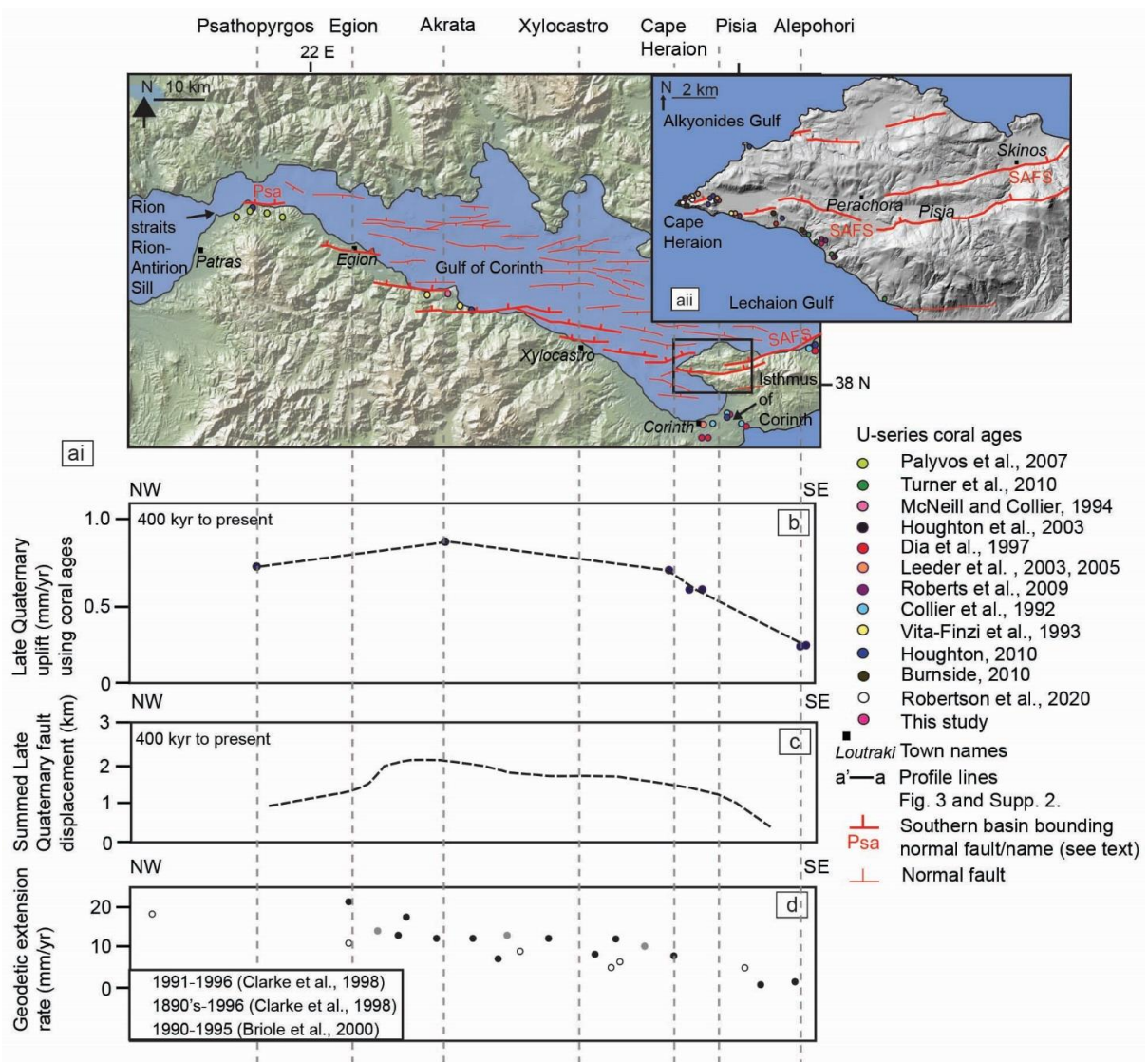
471 4.5 Summary of coral ages and $\delta^{234}\text{U}_i$ findings

472 In summary, our findings suggest that corals from within the Gulf of Corinth with MIS highstand ages
473 (5e, 6d and 7a) have elevated $\delta^{234}\text{U}_i$ reflective of their growth environment, where the hydrochemistry
474 of the gulf deviated from that of the present day. A combination of restricted marine input into the
475 gulf during the highstands and coral growth along fault-controlled margins, where water chemistry
476 was influenced by freshwater, is inferred as the likely cause of elevated $\delta^{234}\text{U}_i$. Whilst tentative values
477 of $\delta^{234}\text{U}_i$ for three Late-Quaternary highstands are suggested, there is likely to be spatial and temporal
478 variation of this value as a result of seasonal and catchment area differences from riverine input. For
479 this reason, coral growth ages are not excluded from this study solely on the basis of the $\delta^{234}\text{U}_i$. Our
480 results are strengthened by the observed stratigraphical and tectonic relationships of Gulf of Corinth
481 corals and other age controls (Supplementary Fig. 2). These findings suggest that where late
482 Quaternary coral ages are obtained from coastal margins or restricted/silled marine basins, age
483 reliability determinations based solely upon $\delta^{234}\text{U}_i$ should be avoided. Coral age reliability should be
484 assessed based upon clustered ages and $\delta^{234}\text{U}_i$ from multiple analyses on the same corallites, in
485 combination with the location of other coral growth ages/age controls relative to the localised
486 tectonic/stratigraphic setting.

487 4.6 Late Quaternary uplift patterns using coral ages

488 Uplift rates on the footwalls of active normal faults that bound the south of the Gulf of Corinth (Fig.
489 1a), calculated using the coral ages discussed herein, can be used to explore Late Quaternary gulf-
490 wide fault-related deformation. East to west along the Gulf of Corinth (Fig. 6), these data show that
491 uplift maxima occur within the central section of the gulf clearly decreasing to the east and appearing
492 to decrease toward the west, though a lack of data prohibits certainty with latter observation (Fig.
493 6b). These results are consistent with summed late Quaternary fault displacement profiles from Bell
494 et al. (2011) (Fig. 6c) who identified a: "...bell-shaped displacement profile with greatest levels of

495 extension in the central part of the rift". Long-term uplift and fault displacement data (Fig. 6b and c)
 496 are not in agreement with short-term geodetic rates of extension (Clarke et al., 1998; Briole et al.,
 497 2000; Bell et al., 2011) (Fig. 6d), which suggest increasing extension from east to west. Detailed
 498 investigations by Bell et al. (2011) led them to hypothesise that this discrepancy may be as a
 499 consequence of variation in the location of maximum extension due to fault growth and linkage. While
 500 the discrepancy between short-term geodetic and long-term fault uplift/displacement rates is
 501 unresolved, it is clear that the age constraints obtained from uplifted corals make a significant
 502 contribution to establishing long-term rates of deformation throughout the Gulf of Corinth.



504 Figure 6: (a) Map of Gulf of Corinth and major faults based upon those used in Nixon et al. (2016). (aii) Perachora peninsula
505 major faults from Roberts et al. (2009). (b) Late Quaternary uplift in the footwall of major north dipping faults that bound
506 the south of the Gulf of Corinth derived from ages of corals from the following studies (west to east): McNeill and Collier,
507 (2004); Houghton et al. (2003); Robertson et al. (2020); Roberts et al. (2009); Houghton (2010); Collier et al. (1992). Uplift
508 values from corals located on the Isthmus of Corinth and eastern Corinth terraces are not plotted as they occur in the back
509 tilted section of the footwall of the South Alkyonides Fault (SAF) and eastern tip of the Xylocastro faults respectively and
510 therefore record minimum uplift values. (c) Summed late Quaternary fault displacement for the Gulf of Corinth, adapted
511 from Bell et al. (2011). (d) Geodetic extension of Clarke et al. (1998) and Briole et al. (2000), adapted from Bell et al. (2011).

512

513 **5. Conclusions**

514 1. Analysis of new and existing coral growth ages suggest that the $\delta^{234}\text{U}_i$ of the Gulf of Corinth
515 during the late Quaternary may be elevated and subject to spatial and temporal variation
516 as a result of the interplay between eustatic sea-level changes, fault controlled
517 uplift/subsidence that limited the marine water ingress into the gulf and freshwater influx
518 from rivers and groundwater.

519 2. The age reliability of corals that have grown along coastal margins and in restricted/semi-
520 restricted marine environments should not be solely evaluated on the basis of the $\delta^{234}\text{U}_i$
521 relative to open ocean values. Rather, we suggest that corallites from the same layer are
522 analysed and that multiple analyses on the same corallites may be useful to determine age
523 and $\delta^{234}\text{U}_i$ reliability, in combination with consideration of the stratigraphic and tectonic
524 setting of the corals and their relative position to other age constraints.

525 3. Coral ages along the southern margin of the Gulf of Corinth provide a reliable means to
526 explore long-term uplift patterns and are in agreement with other geological measurements
527 such as late Quaternary fault displacement profiles.

528

529 **Acknowledgements**

530 $^{234}\text{U}/^{230}\text{Th}$ coral age dating was carried out at the Geochronology and Tracers Facility (BGS, UK) and
531 funded via grant IP-1734-0517.

532 Data availability

533 All data for this paper are appropriately cited and referred to in the reference list and available from

534 Tables 2 and Supplementary Table 1. These data can be used to reproduce the results.

535

536 Andersen, M.B., Stirling, C.H., Porcelli, D., Halliday, A.N., Andersson, P.S. and Baskaran, M., 2007. The
537 tracing of riverine U in Arctic seawater with very precise $^{234}\text{U}/^{238}\text{U}$ measurements. *Earth and*
538 *Planetary Science Letters*, 259(1-2), pp.171-185.

539 Andersson, P.S., Wasserburg, G.J., Chen, J.H., Papanastassiou, D.A. and Ingri, J., 1995. $^{238}\text{U}/^{234}\text{U}$
540 and $^{232}\text{Th}/^{230}\text{Th}$ in the Baltic Sea and in river water. *Earth and Planetary Science Letters*, 130(1-4),
541 pp.217-234.

542 Bard, E., Fairbanks, R.G., Hamelin, B., Zindler, A. and Hoang, C.T., 1991. Uranium-234 anomalies in
543 corals older than 150,000 years. *Geochimica et Cosmochimica Acta*, 55(8), pp.2385-2390.

544 Bard, E., Jouannic, C., Hamelin, B., Pirazzoli, P., Arnold, M., Faure, G. and Sumosusastro, P., 1996.
545 Pleistocene sea levels and tectonic uplift based on dating of corals from Sumba Island, Indonesia.
546 *Geophysical Research Letters*, 23(12), pp.1473-1476.

547 Bell, R.E., McNeill, L.C., Henstock, T.J. and Bull, J.M., 2011. Comparing extension on multiple time
548 and depth scales in the Corinth Rift, Central Greece. *Geophysical Journal International*, 186(2),
549 pp.463-470.

550 Briole, P., Rigo, A., Lyon-Caen, H., Ruegg, J.C., Papazissi, K., Mitsakaki, C., Balodimou, A., Veis, G.,
551 Hatzfeld, D. and Deschamps, A., 2000. Active deformation of the Corinth rift, Greece: results from
552 repeated Global Positioning System surveys between 1990 and 1995. *Journal of Geophysical*
553 *Research: Solid Earth*, 105(B11), pp.25605-25625.

554 Bryant, J.D., Jones, D.S. and Mueller, P.A., 1995. Influence of freshwater flux on $^{87}\text{Sr}/^{86}\text{Sr}$
555 chronostratigraphy in marginal marine environments and dating of vertebrate and invertebrate
556 faunas. *Journal of Paleontology*, pp.1-6.

557

558 Burke, W.H., Denison, R.E., Hetherington, E.A., Koepnick, R.B., Nelson, H.F. and Otto, J.B., 1982.
559 Variation of seawater $^{87}\text{Sr}/^{86}\text{Sr}$ throughout Phanerozoic time. *Geology*, 10(10), pp.516-519.

560

561 Burnside, 2010. Unpublished Thesis. University of Glasgow.

562 Cheng, H., Edwards, R.L., Shen, C.C., Polyak, V.J., Asmerom, Y., Woodhead, J., Hellstrom, J., Wang, Y.,
563 Kong, X., Spötl, C. and Wang, X., 2013. Improvements in ^{230}Th dating, ^{230}Th and ^{234}U half-life
564 values, and U–Th isotopic measurements by multi-collector inductively coupled plasma mass
565 spectrometry. *Earth and Planetary Science Letters*, 371, pp.82-91.

- 566 Chutcharavan, P.M., Dutton, A. and Ellwood, M.J., 2018. Seawater 234U/238U recorded by modern
567 and fossil corals. *Geochimica et Cosmochimica Acta*, 224, pp.1-17.
- 568 Clarke, P.J., Davies, R.R., England, P.C., Parsons, B., Billiris, H., Paradissis, D., Veis, G., Cross, P.A.,
569 Denys, P.H., Ashkenazi, V. and Bingley, R., 1998. Crustal strain in central Greece from repeated GPS
570 measurements in the interval 1989–1997. *Geophysical Journal International*, 135(1), pp.195-214.
- 571 Collier, R.L., Leeder, M.R., Rowe, P.J. and Atkinson, T.C., 1992. Rates of tectonic uplift in the Corinth
572 and Megara basins, central Greece. *Tectonics*, 11(6), pp.1159-1167.
- 573 Collier, R.E.L. and Thompson, J., 1991. Transverse and linear dunes in an Upper Pleistocene marine
574 sequence, Corinth Basin, Greece. *Sedimentology*, 38(6), pp.1021-1040.
- 575 Crémière, A., Lepland, A., Chand, S., Sahy, D., Condon, D.J., Noble, S.R., Martma, T., Thorsnes, T.,
576 Sauer, S. and Brunstad, H., 2016. Timescales of methane seepage on the Norwegian margin
577 following collapse of the Scandinavian Ice Sheet. *Nature communications*, 7(1), pp.1-10.
- 578 Dia, A.N., Cohen, A.S., O'nions, R.K. and Jackson, J.A., 1997. Rates of uplift investigated through
579 230Th dating in the Gulf of Corinth (Greece). *Chemical Geology*, 138(3-4), pp.171-184.
- 580 Dutton, A., 2015. Uranium-thorium dating. *Handbook of sea-level research*. Chichester: John Wiley &
581 Sons, Ltd, pp.386-403.
- 582 Dutton, A., Bard, E., Antonioli, F., Esat, T.M., Lambeck, K. and McCulloch, M.T., 2009. Phasing and
583 amplitude of sea-level and climate change during the penultimate interglacial. *Nature Geoscience*,
584 2(5), pp.355-359.
- 585 Dutton, A., Webster, J.M., Zwartz, D., Lambeck, K. and Wohlfarth, B., 2015. Tropical tales of polar ice:
586 evidence of Last Interglacial polar ice sheet retreat recorded by fossil reefs of the granitic Seychelles
587 islands. *Quaternary Science Reviews*, 107, pp.182-196.
- 588 Edwards, R.L., Chen, J.H. and Wasserburg, G.J., 1987. 238U234U230Th232Th systematics and the
589 precise measurement of time over the past 500,000 years. *Earth and Planetary Science Letters*, 81(2-
590 3), pp.175-192.
- 591 Esat, T.M. and Yokoyama, Y., 2010. Coupled uranium isotope and sea-level variations in the oceans.
592 *Geochimica et Cosmochimica Acta*, 74(24), pp.7008-7020.
- 593 Gallup, C.D., Cheng, H., Taylor, F.W. and Edwards, R.L., 2002. Direct determination of the timing of
594 sea level change during Termination II. *Science*, 295(5553), pp.310-313.
- 595 Grant, K.M., Rohling, E.J., Ramsey, C.B., Cheng, H., Edwards, R.L., Florindo, F., Heslop, D., Marra, F.,
596 Roberts, A.P., Tamisiea, M.E. and Williams, F., 2014. Sea-level variability over five glacial cycles.
597 *Nature communications*, 5(1), pp.1-9.
- 598
599 Grant, L.B., Mueller, K.J., Gath, E.M., Cheng, H., Lawrence Edwards, R., Munro, R. and Kennedy, G.L.,
600 1999. Late Quaternary uplift and earthquake potential of the San Joaquin Hills, southern Los Angeles
601 basin, California. *Geology*, 27(11), pp.1031-1034.

602
603 Grzymko, T.J., Marcantonio, F., McKee, B.A. and Stewart, C.M., 2007. Temporal variability of uranium
604 concentrations and $^{234}\text{U}/^{238}\text{U}$ activity ratios in the Mississippi river and its tributaries. *Chemical*
605 *Geology*, 243(3-4), pp.344-356.

606 Hamelin, B., Bard, E., Zindler, A. and Fairbanks, R.G., 1991. $^{234}\text{U}/^{238}\text{U}$ mass spectrometry of corals:
607 How accurate is the UTh age of the last interglacial period?. *Earth and Planetary Science Letters*,
608 106(1-4), pp.169-180.

609 Henderson, G.M., Martel, D.J., O'Nions, R.K. and Shackleton, N.J., 1994. Evolution of seawater
610 $^{87}\text{Sr}/^{86}\text{Sr}$ over the last 400 ka: the absence of glacial/interglacial cycles. *Earth and Planetary Science*
611 *Letters*, 128(3-4), pp.643-651.

612 Hodell, D.A., Mead, G.A. and Mueller, P.A., 1990. Variation in the strontium isotopic composition of
613 seawater (8 Ma to present): Implications for chemical weathering rates and dissolved fluxes to the
614 oceans. *Chemical Geology: Isotope Geoscience section*, 80(4), pp.291-307.

615 Houghton, S.L., Roberts, G.P., Papanikolaou, I.D., McArthur, J.M. and Gilmour, M.A., 2003. New
616 ^{234}U - ^{230}Th coral dates from the western Gulf of Corinth: Implications for extensional tectonics.
617 *Geophysical Research Letters*, 30(19).

618 Houghton, 2010. Unpublished Thesis. Birkbeck College, University of London.

619 Krabbenhöft, A., Eisenhauer, A., Böhm, F., Vollstaedt, H., Fietzke, J., Liebetrau, V., Augustin, N.,
620 Peucker-Ehrenbrink, B., Müller, M.N., Horn, C. and Hansen, B.T., 2010. Constraining the marine
621 strontium budget with natural strontium isotope fractionations ($^{87}\text{Sr}/^{86}\text{Sr}^*$, $\delta^{88}/^{86}\text{Sr}$) of
622 carbonates, hydrothermal solutions and river waters. *Geochimica et Cosmochimica Acta*, 74(14),
623 pp.4097-4109.

624 Leeder, M.R., McNeill, L.C., Li Collier, R.E., Portman, C., Rowe, P.J., Andrews, J.E. and Gawthorpe,
625 R.L., 2003. Corinth rift margin uplift: New evidence from Late Quaternary marine shorelines.
626 *Geophysical Research Letters*, 30(12).

627 Leeder, M.R., Portman, C., Andrews, J.E., Collier, R.L., Finch, E., Gawthorpe, R.L., McNeill, L.C., Perez-
628 Arlucea, M. and Rowe, P., 2005. Normal faulting and crustal deformation, Alkyonides Gulf and
629 Perachora peninsula, eastern Gulf of Corinth rift, Greece. *Journal of the Geological Society*, 162(3),
630 pp.549-561

631 Luijendijk, E., Gleeson, T. and Moosdorf, N., 2020. Fresh groundwater discharge insignificant for the
632 world's oceans but important for coastal ecosystems. *Nature communications*, 11(1), pp.1-12.

633 McNeill, L.C. and Collier, R.L., 2004. Uplift and slip rates of the eastern Eliki fault segment, Gulf of
634 Corinth, Greece, inferred from Holocene and Pleistocene terraces. *Journal of the Geological Society*,
635 161(1), pp.81-92.

636 McNeill, L.C., Shillington, D.J., Carter, G.D., Everest, J.D., Gawthorpe, R.L., Miller, C., Phillips, M.P.,
637 Collier, R.E.L., Cvetkoska, A., De Gelder, G. and Diz, P., 2019. High-resolution record reveals climate-
638 driven environmental and sedimentary changes in an active rift. *Scientific reports*, 9(1), pp.1-11.

- 639 Medina-Elizalde, M., 2013. A global compilation of coral sea-level benchmarks: implications and new
640 challenges. *Earth and Planetary Science Letters*, 362, pp.310-318.
- 641 Muhs, D.R., Kennedy, G.L. and Rockwell, T.K., 1994. Uranium-series ages of marine terrace corals
642 from the Pacific coast of North America and implications for last-interglacial sea level history.
643 *Quaternary Research*, 42(1), pp.72-87.
- 644 Nixon, C.W., McNeill, L.C., Bull, J.M., Bell, R.E., Gawthorpe, R.L., Henstock, T.J., Christodoulou, D.,
645 Ford, M., Taylor, B., Sakellariou, D. and Ferentinos, G., 2016. Rapid spatiotemporal variations in rift
646 structure during development of the Corinth Rift, central Greece. *Tectonics*, 35(5), pp.1225-1248.
- 647 Palmer, M.R. and Edmond, J.M., 1993. Uranium in river water. *Geochimica et Cosmochimica Acta*,
648 57(20), pp.4947-4955.
- 649 Palyvos, N., Mancini, M., Sorel, D., Lemeille, F., Pantosti, D., Julia, R., Triantaphyllou, M. and De
650 Martini, P.M., 2010. Geomorphological, stratigraphic and geochronological evidence of fast
651 Pleistocene coastal uplift in the westernmost part of the Corinth Gulf Rift (Greece). *Geological*
652 *Journal*, 45(1), pp.78-104.
- 653 Papanikolaou, I.D., Triantaphyllou, M., Pallikarakis, A. and Migiros, G., 2015. Active faulting at the
654 Corinth Canal based on surface observations, borehole data and paleoenvironmental
655 interpretations. Passive rupture during the 1981 earthquake sequence?. *Geomorphology*, 237,
656 pp.65-78.
657
- 658 Peirano, A., Morri, C., Bianchi, C.N., Aguirre, J., Antonioli, F., Calzetta, G., Carobene, L., Mastronuzzi,
659 G. and Orrù, P., 2004. The Mediterranean coral *Cladocora caespitosa*: a proxy for past climate
660 fluctuations?. *Global and planetary Change*, 40(1-2), pp.195-200.
661
- 662 Perissoratis, C., Piper, D.J.W. and Lykousis, V., 2000. Alternating marine and lacustrine sedimentation
663 during late Quaternary in the Gulf of Corinth rift basin, central Greece. *Marine Geology*, 167(3-4),
664 pp.391-411.
- 665 Roberts, G.P., Houghton, S.L., Underwood, C., Papanikolaou, I., Cowie, P.A., van Calsteren, P., Wigley,
666 T., Cooper, F.J. and McArthur, J.M., 2009. Localization of Quaternary slip rates in an active rift in 105
667 years: An example from central Greece constrained by ²³⁴U-²³⁰Th coral dates from uplifted
668 paleoshorelines. *Journal of Geophysical Research: Solid Earth*, 114(B10).
- 669 Robertson, J., Roberts, G.P., Iezzi, F., Meschis, M., Gheorghiu, D.M., Sahy, D., Bristow, C. and
670 Sgambato, C., 2020. Distributed normal faulting in the tip zone of the South Alkyonides Fault System,
671 Gulf of Corinth, constrained using ³⁶Cl exposure dating of Late-Quaternary wave-cut platforms.
672 *Journal of Structural Geology*, p.104063.
- 673 Rohling, E.J., Fenton, M.J.J.F., Jorissen, F.J., Bertrand, P., Ganssen, G. and Caulet, J.P., 1998.
674 Magnitudes of sea-level lowstands of the past 500,000 years. *Nature*, 394(6689), pp.162-165.
- 675 Siddall, M., Rohling, E.J., Almogi-Labin, A., Hemleben, C., Meischner, D., Schmelzer, I. and Smeed,
676 D.A., 2003. Sea-level fluctuations during the last glacial cycle. *Nature*, 423(6942), pp.853-858.

- 677 Sieh, K., Natawidjaja, D.H., Meltzner, A.J., Shen, C.C., Cheng, H., Li, K.S., Suwargadi, B.W., Galetzka, J.,
678 Philibosian, B. and Edwards, R.L., 2008. Earthquake supercycles inferred from sea-level changes
679 recorded in the corals of west Sumatra. *Science*, 322(5908), pp.1674-1678.
- 680 Shen, G.T. and Dunbar, R.B., 1995. Environmental controls on uranium in reef corals. *Geochimica et*
681 *Cosmochimica Acta*, 59(10), pp.2009-2024.
- 682 Soter, S., Blackwelder, P., Tziavos, C., Katsonopoulou, D., Hood, T. and Alvarez-Zarikian, C., 2001.
683 Environmental analysis of cores from the Helike Delta, Gulf of Corinth, Greece. *Journal of Coastal*
684 *Research*, pp.95-106. .
- 685 Turner, J.A., Leeder, M.R., Andrews, J.E., Rowe, P.J., Van Calsteren, P. and Thomas, L., 2010. Testing
686 rival tectonic uplift models for the Lechaion Gulf in the Gulf of Corinth rift. *Journal of the Geological*
687 *Society*, 167(6), pp.1237-1250.
- 688 van Calsteren, P. and Thomas, L., 2006. Uranium-series dating applications in Natural Environmental
689 Science. *Earth-Science Reviews*, 75(1-4), pp.155-175.
- 690 Vita-Finzi, C., 1993. Evaluating late Quaternary uplift in Greece and Cyprus. *Geological Society,*
691 *London, Special Publications*, 76(1), pp.417-424.
- 692 Watkins, S.E., Whittaker, A.C., Bell, R.E., Brooke, S.A., Ganti, V., Gawthorpe, R.L., McNeill, L.C. and
693 Nixon, C.W., 2020. Straight from the source's mouth: Controls on field-constrained sediment export
694 across the entire active Corinth Rift, central Greece. *Basin Research*, 32(6), pp.1600-1625.
- 695 Zunino, S., Pitacco, V., Mavrič, B., Orlando-Bonaca, M., Kružić, P. and Lipej, L., 2018. The ecology of
696 the Mediterranean stony coral *Cladocora caespitosa* (Linnaeus, 1767) in the Gulf of Trieste (northern
697 Adriatic Sea): a 30-year long story. *Marine Biology Research*, 14(3), pp.307-320.
- 698
- 699